Observation of Covalent Intermediates in an Enzyme Mechanism at Atomic Resolution

Andreas Heine, *et al.*

Science **294**, 369 (2001);
DOI: 10.1126/science.1063601

Observation of Covalent Intermediates in an Enzyme Mechanism at Atomic Resolution

Andreas Heine,[1]* Grace DeSantis,[2]*† John G. Luz,[1] Michael Mitchell,[2] Chi-Huey Wong[2,3]‡ Ian A. Wilson[1,3]‡

In classical enzymology, intermediates and transition states in a catalytic mechanism are usually inferred from a series of biochemical experiments. Here, we derive an enzyme mechanism from true atomic-resolution x-ray structures of reaction intermediates. Two ultra–high resolution structures of wild-type and mutant D-2-deoxyribose-5-phosphate (DRP) aldolase complexes with DRP at 1.05 and 1.10 angstroms unambiguously identify the postulated covalent carbinolamine and Schiff base intermediates in the aldolase mechanism. In combination with site-directed mutagenesis and ^{1}H nuclear magnetic resonance, we can now propose how the heretofore elusive C-2 proton abstraction step and the overall stereochemical course are accomplished. A proton relay system appears to activate a conserved active-site water that functions as the critical mediator for proton transfer.

Escherichia coli D-2-deoxyribose-5-phosphate aldolase (DERA, E.C. 4.1.2.4) catalyzes the reversible aldol reaction between the donor aldehyde, acetaldehyde, and the acceptor substrate, D-glyceraldehyde-3-phosphate, to generate D-2-deoxyribose-5-phosphate (DRP) (Fig. 1) (*1*). *E. coli* DERA belongs to the type I class of aldolases, which use a covalent Schiff base intermediate during catalysis (*2*–*4*), and is one of the most efficient among known aldolases (*5*–*7*). DERA is unique in catalyzing an aldol reaction between two aldehydes, and its broad substrate specificity confers considerable utility as a biocatalyst (*5*), offering an environmentally benign alternative to chiral transition metal catalysis of the asymmetric aldol reaction (*8*, *9*). The synthetic utility of aldolases in C–C bond-forming reactions is also apparent from extensive efforts to generate catalytic antibodies that catalyze aldol reactions (*10*–*14*).

Despite their initial characterization at the turn of the past century, catalytic mechanisms for class I aldolases have remained speculative because of the lack of high-resolution complex structures and incomplete kinetic data (*15*–*17*). Furthermore, the identity of the general base that generates the nucleophilic enamine intermediate has remained elusive (*7*, *18*). Proposed mechanisms for three fructose 1,6-bisphosphate aldolases (FBPs) have been based on noncovalent substrate and product complexes (*7*, *19*, *20*). The only known covalent complex structures are for an adduct of pyruvate with D-2-keto-3-deoxy-6-phosphogluconate (KDPG) aldolase (*17*) and for dihydroxyacetone in complex with transaldolase B (*21*). These studies have identified the Schiff base–forming lysine, which is normally located on strand β6, but the general acid and base residues required by the aldolase mechanism have not been unambiguously characterized (*7*, *15*, *16*, *18*, *19*, *22*). In previous mechanisms, glutamic or aspartic acid have often been proposed to act as general acids or bases. [Further discussion of other proposed catalytic residues is found in the supplemental material (*22*).]

A covalent complex of DERA with DRP was obtained by soaking crystals with the substrate just before data collection [for further details, see the supplemental material and Web fig. 2 (*22*)]. An ultra–high resolution data set was then collected at 1.05 Å resolution (Table 1). The overall enzyme structure adopts the classic TIM barrel $(\alpha/\beta)_8$ fold, with Lys^{167} on strand β6 [see Web fig. 1 (*22*)]. The covalently bound substrate protrudes out of the binding pocket, with its phosphate moiety ligand in close proximity to the COOH-terminal α helix (*23*). A search of the Cambridge Structural Database did not find any crystal structure for DRP, either in its linear or cyclic form. However, the advantage of ultra–high resolution data is that the ligand atoms can be individually placed and refined into the electron density (Fig. 2A). Coordinates for the covalently bound carbinolamine were therefore obtained from a free atom model by applying the structure extension mode available in SHELXL (Table 1). Geometric restraints were not applied for the ligand in the final stages of refinement; hence, the ultra–high resolution data allowed for an unrestrained refinement of the Lys Nζ–C1 DRP bond length (1.38 Å) for both complexes in the crystal asymmetric unit (Fig. 2B). The substrate carbonyl C=O bond, which is typically between 1.2 to 1.25 Å for small molecules, refined to 1.39 Å (Fig. 2B) and 1.35Å in the two complexes, clearly indicating the presence of a hydroxyl group.

Thus, the atomic refinement identified the formation of a carbinolamine, which is the first covalent intermediate expected in the reaction of an aldehyde with a lysine. A second lysine, Lys^{201}, is only 3.4 Å from Lys^{167}, with Asp^{102} forming a bridge between them (Fig. 3A). Lys^{201} forms another buried salt bridge with Asp^{16}, which is held in place by Arg^{234}. This latter salt bridge

[1]Department of Molecular Biology, [2]Department of Chemistry, [3]Skaggs Institute for Chemical Biology, The Scripps Research Institute, 10550 North Torrey Pines Road, La Jolla, CA 92037, USA.

*These authors contributed equally to this work.
†Present address: Diversa Corporation, 4955 Directors Place, San Diego, CA 92121, USA.
‡To whom correspondence should be addressed. E-mail: wong@scripps.edu (C.-H.W.); wilson@scripps.edu (I.A.W.)

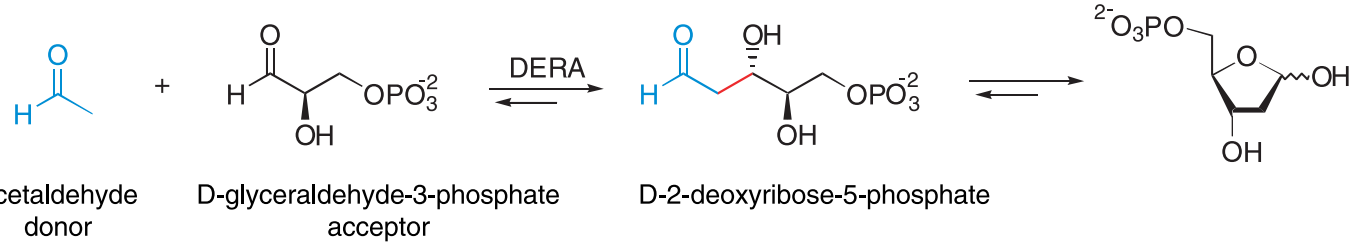

Fig. 1. DERA reaction. In vivo, DERA catalyzes the aldol reaction between the acetaldehyde donor and D-glyceraldehyde-3-phosphate acceptor to generate DRP.

may be important for maintenance of a positive charge on Lys^{201} that results in a lowering of the pK_a of Lys^{167} through electrostatic interaction. The uncharged Lys^{167} then functions as a nucleophile at neutral pH by attacking the substrate carbonyl carbon. The substrate carbonyl oxygen may be further activated by interaction with a structurally conserved active-site water molecule, Wat^{29} (Figs. 2B and 3A) (*24*). Comparison with other known class I aldolase structures (*22*, *25*) shows that a similar constellation of key catalytic residues appears to be present in their active sites, but their precise configuration differs from enzyme to enzyme, suggesting that the aldolase mechanism does not require a unique geometric arrangement of catalytic residues.

Several mutants were then designed to investigate the catalytic roles for the Schiff base Lys^{167} and potential acid or base residues (Table 2). Because the $Lys^{201} \rightarrow Leu^{201}$ (K201L) mutant was essentially inactive (*26*), we assumed that this mutant would allow further evaluation of possible covalent intermediates. Its structure in complex with DRP was determined at 1.10 Å resolution (Table 1) and revealed a different covalent intermediate; the absence of any electron density for a C1-hydroxyl group (Fig. 2C) indicated formation of a covalent Schiff base rather than the carbinolamine. The K201L mutant may then be unable to execute the proton relay role proposed for Lys^{201}, and thus the Schiff base presumably becomes trapped because of the relative free energy differences of the enzyme-bound intermediates. The DRP C1–Lys Nζ atom distance could again be refined in this structure and was found to be 1.29 Å (Fig. 2C) and 1.28 Å, respectively (for the two independent complexes in the asymmetric unit), without use of any geometric restraints on the ligand. This decrease of 0.1 Å in bond length clearly indicates at least partial double-bond character and, therefore, a true Schiff base complex. The shorter Nζ–C bond and an Nζ–C–C angle of 125.0° for the Schiff base specifies trigonal geometry at the carbon atom (C1), which is in excellent agreement with the theoretical values. Furthermore, the observed bond angles for the DERA wild-type carbinolamine complex also agree well with theoretical values and, in this case, indicate a tetrahedral arrangement around the C1 of the substrate. [For comparison with the KDPG pyruvate carbinolamine complex, see the supplemental material (*22*).]

Site-directed mutagenesis of the two DERA active site lysine residues Lys^{167} and Lys^{201} indicate that both are critical to catalysis. The K167L and K201L mutants are both 10^3 times less active than the wild type (Table 2). However, the K201L mutant structure (Fig. 2C) shows that Lys^{201} is not obligatory for Schiff base formation (*27*), although it substantially enhances the rate of reaction. A likely function of Lys^{201} is to lower the pK_a of Lys^{167} and raise its nucleophilicity by the classical Westheimer mechanism first proposed for acetoacetate decarboxylase (*28*, *29*). The pH activity profile for wild-type DERA has an inflection point with a pK_a of 6.8 that may be ascribed to the ionization of Lys^{167} (*30*). By contrast, in the aldolase-catalyzing abzyme Ab38C2, insertion of the Schiff base lysine into a hydrophobic pocket lowers its pK_a to 6.0 (*11*). However, because the $Lys^{201} \rightarrow Arg^{201}$ (K201R) mutant of DERA is also inactive, the role of Lys^{201} is clearly more than a simple electrostatic one (*31*).

The K167R mutant is only 22 times less active than the wild type; thus, in this case, Lys^{201} might assume the role of Lys^{167}, as proposed for the KDPG aldolase double mutant (*15*). Calculation of the solvent-accessible surface area (*32*) of wild-type

Table 1. Data collection and refinement statistics. The DERA enzyme (10 to 15 mg/ml) crystallizes at 4°C from 13 to 18% MPEG5000, 0.1 M cacodylate (pH5.5), and 15 to 20% glycerol with two molecules in the asymmetric unit (*34*). The complexes were obtained by short soaks with the substrate immediately before flash cooling in 10.6 mM substrate concentration. All data sets were collected at SSRL beamline 9-2 at –176°C. Data were processed and scaled with HKL2000 (*51*). The native structure of DERA was used as a starting model for refinement (*34*). The initial refinement in CNS (*52*) used rigid-body, positional, and slow-cooling refinement protocols. Refinement of the ultra–high resolution complexes was continued with SHELXL-97 (*53*). For each refinement step, at least 10 cycles of conjugate gradient minimization were performed, with restraints on bond distances, angles, and B values. In the final stages, hydrogen atoms were placed in calculated positions without use of additional parameters. Intermittent cycles of model building were done with the program O (*54*). The overall map quality was excellent, showing no main-chain breaks, except for one region of weaker density (residues 22 to 23), which is observed in all DERA structures. At the COOH-terminus, 8 to 9 residues were not visible in the electron density, presumably because of disorder, as observed for other aldolase structures (*7*, *55*, *56*). The only outlier in the Ramachandran plot, as assessed by Procheck (*57*), is residue Lys^{146}, as observed in all DERA structures, that is in a well-defined γ-turn with excellent density. The bond length (that is, the corresponding atom positions) for Lys^{167} Nζ to C1 of the substrate, and C1 to O1 in the wild-type complex, were refined without any restraints in all stages of refinement. The carbinolamine atoms were positioned as individual water molecules during initial SHELXL refinement. All atoms for the ligand were identified and placed into corresponding electron density peaks. No geometric restraints were used in late stages of refinement for the bound substrate molecules and estimated standard deviations (esd's) were determined in the last cycle of refinement.

	Wild-type complex	K201L mutant complex
Resolution range (Å)	30–1.05	20–1.10
Space group	$P2_1$	$P2_1$
Unit cell (Å,° for β)	a = 48.5, b = 42.0, c = 145.0, β = 98.4	a = 48.6, b = 42.0, c = 145.4, β = 98.4
Highest resolution shell (Å)	1.07–1.05	1.12–1.10
No. of observations	638,223	426,815
No. of unique reflections	256,887	218,336
Completeness (%)	95.5 [64.0]*	93.2 [78.9]*
Mean I/σ_I	14.8 [1.0]	16.2 [1.6]
R_{sym} (%)†	6.3 [66.7]	5.4 [50.5]
Refined residues	503	503
Refined substrate atoms	26	24
Refined water molecules	708	557
Resolution range in refinement (Å)	10.0–1.05	8.0–1.10
R_{cryst} ($F_o > 4\sigma F_o$; F_o)‡	11.0; 14.3	12.4; 14.2
R_{free} ($F_o > 4\sigma F_o$; F_o)§	13.5; 16.9	14.6; 16.8
Rms deviations		
Bond lengths (Å)	0.015	0.014
Bond angles (°)	2.2	2.2
Average B value (Å²) (mol1; 2)	11.7; 12.4	13.0; 13.8
Main chain (Å²)	9.4; 10.0	10.3; 10.9
Side chain (Å²)	14.2; 15.2	16.1; 17.0
Substrate (Å²)	11.9; 14.4	8.3; 9.5
Waters (Å²)	28.5	28.1
Ramachandran plot‖		
Most favored (%)	94.7	95.8
Additional allowed (%)	4.4	3.3
Generously allowed (%)	0.4	0.4
Disallowed (%)	0.4	0.4

*Values in brackets are statistics for the highest resolution shell. †$R_{sym} = [\Sigma_h \Sigma_i |I_i(h) - \langle I(h)\rangle| / \Sigma_h \Sigma_i I_i(h)] \times 100$, where $\langle I(h)\rangle$ is the mean of the $I(h)$ observation of reflection h. ‡$R_{cryst} = \Sigma_{hkl} |F_o - F_c| / \Sigma_{hkl} |F_o|$. §$R_{free}$ was calculated as for R_{cryst} but on 5% of the data excluded from the refinement. ‖From Procheck (*57*).

DERA shows that only 24 Å^2 of the Lys^{167} side chain and none of Lys^{201} are solvent-exposed. However, substitution of Lys^{167} with arginine would still result in complete burial of Lys^{201}, whereas in the K167L mutant, only 11Å^2 of the Lys^{201} would be solvent-exposed. However, no Schiff base intermediate between acetaldehyde and DERA K167R could be trapped after sodium borohydride reduction (*33*).

The second critical residue for a Schiff base–mediated aldol reaction is a general base that deprotonates the imine to form an enamine. However, no obvious protein side chain candidate is apparent from these DERA structures. Cys^{47} is conserved in 13 of the 15 known DERA sequences, and from the native uncomplexed structure, we initially thought that it might fulfill this role (*34*). However, the Cys^{47} → Ala^{47} and Cys^{47} → Ser^{47} mutants are only slightly less active than the wild type. In addition, in the wild-type carbinolamine complex structure (Fig. 3B), the S_β atom of Cys^{47} is too far (5.4 to 5.5Å) from the C2 atom of DRP.

Mechanistic studies have suggested that the side-chain hydroxyl of a COOH-terminal tyrosine residue found in many type I aldolases might function as the C2 proton-abstracting general base (*7*, *19*, *35*). Carboxypeptidase cleavage of the COOH-terminal tyrosine of *Salmonella typhimurium* DERA resulted in a substantially less active enzyme, but it was still able to bind substrate (*4*, *36*). Because the eight to nine COOH-terminal residues of DERA were not visible in the electron density, a minimized model was constructed that indicated that Tyr^{259} could reach into the active site (*37*). Because the Tyr^{259} → Phe^{259} (Y259F) mutant exhibited only a 200-fold decrease in activity (Table 2), its potential role as a general base could not be validated from mutagenesis or from the crystal structures.

To further address this question, we turned to ^{1}H nuclear magnetic resonance (NMR), which permits direct monitoring of the enzyme-catalyzed deprotonation of the C2 proton. Even in the absence of an acceptor substrate, DERA catalyzes the exchange of the C2 protons of the natural donor acetaldehyde or its homolog propanaldehyde (*38*). Although DERA catalyzes the exchange of all three C2 protons of acetaldehyde, presumably because of free rotation about the C1–C2 bond in the ES complex, only one of the two prochiral C2 protons of propanaldehyde is exchanged. The DERA-catalyzed exchange of the C2 proton is readily monitored by ^{1}H NMR, when conducted in D_2O triethanolamine buffer. ^{1}H NMR studies revealed that both wild-type DERA and the Y259F mutant catalyze the C2 exchange of one of the prochiral C2 protons of propanaldehyde (Table 2), thus eliminating any role for the tyrosine side chain as a general base. Furthermore, in the DERA-catalyzed C2 exchange reaction of both (*R*)-2-deuteropro-

Table 2. Activity of DERA mutants. n.d., not determined.

Mutant*	K_{cat} (s^{-1})†	K_M (mM)	k_{cat}/K_M (s^{-1} mM^{-1})	C-2 exchange‡ (by ^{1}H NMR)
Wild type	68 ± 1	0.64 ± 0.01	106 ± 2	Yes
K167L	0.063 ± 0.002	0.64 ± 0.08	0.1 ± 0.01	No
K167R	1.65 ± 0.07	0.34 ± 0.05	4.9 ± 0.7	No
K201R	0.022 ± 0.002	0.22 ± 0.02	0.1 ± 0.01	No
K201L	0.0195 ± 0.0007	0.28 ± 0.04	0.07 ± 0.01	No
K137L	1.54 ± 0.03	0.31 ± 0.03	5.0 ± 0.5	n.d.
C47A	9.4 ± 0.03	0.22 ± 0.03	43 ± 5	n.d.
C47S	7.9 ± 0.3	0.23 ± 0.03	34 ± 4	n.d.
D102N	0.0144 ± 0.006	0.21 ± 0.04	0.07 ± 0.01	No
D102E	0.68 ± 0.04	0.28 ± 0.07	2.4 ± 0.6	Yes
D102L	0.005 ± 0.001	0.10 ± 0.02	0.05 ± 0.01	No
Y259F	0.164 ± 0.004	0.31 ± 0.03	0.53 ± 0.05	Yes

*All enzymes were expressed from the pET30a plasmid in *E. coli* BL21 (*DE3*) as NH_2-terminal HIS_6 fusions and purified to homogeneity by Ni^{2+}-agarose affinity chromatography. †Enzyme activity was assayed in the retroaldol direction with 0.01 to 4 mM DRP in 50 mM (pH 7.5) TEA-HCl buffer using a GPD/TPI (1.6 U/ml Sigma G-1881) coupled enzyme system at 25°C in the presence of 0.3 mM NADH by observing the rate of decrease of NADH concentration as monitored by absorption at 340 nm (*58*). ‡200 mM propanaldehyde was incubated in 50 mM TEA-HCl buffer made up to pD 7.1 and then 0.5 to 2 mg of DERA was added. ^{1}H NMRs were recorded on a 250-MHz Bruker (*59*).

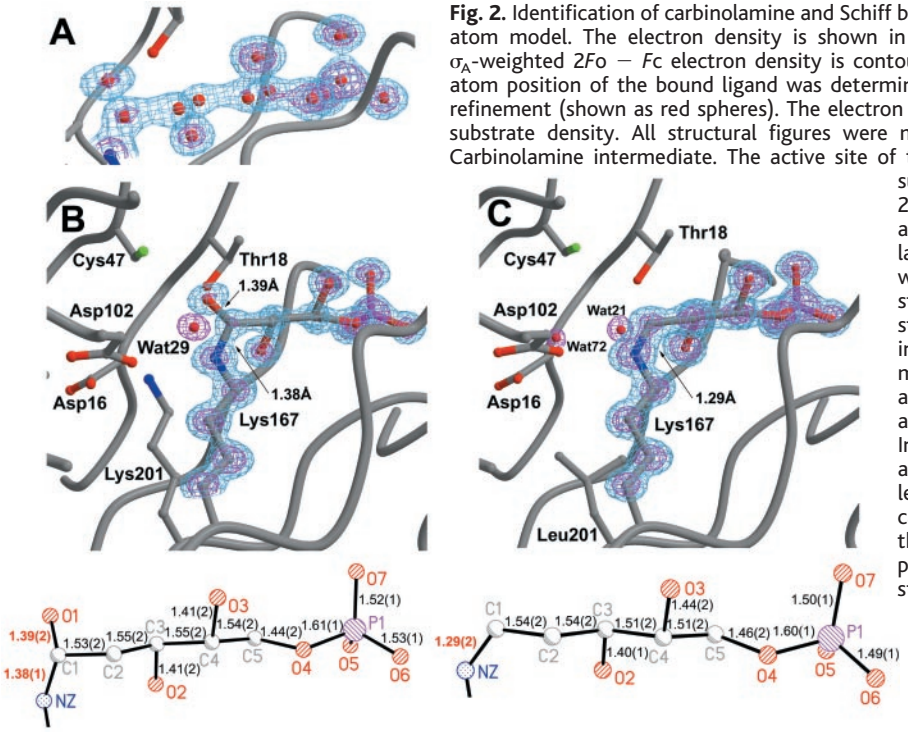

Fig. 2. Identification of carbinolamine and Schiff base intermediates. (**A**) Ligand construction from free atom model. The electron density is shown in the DERA active site for the carbinolamine. The σ_A-weighted 2*Fo* − *Fc* electron density is contoured at 2σ (cyan) and 4σ (purple). Each individual atom position of the bound ligand was determined iteratively and placed into electron density for refinement (shown as red spheres). The electron density for Lys^{167} is displayed for comparison with substrate density. All structural figures were made with Bobscript (*60*) and Raster3D (*61*). (**B**) Carbinolamine intermediate. The active site of the wild-type DERA enzyme in complex with DRP substrate is shown around Lys^{167}. The σ_A-weighted 2*Fo* − *Fc* electron density is contoured at 2σ (cyan) and 4σ (purple). Formation of the covalent carbinolamine is observed. Active site residues are labeled as well as the active site water, Wat^{29}. Below: Unrestrained refinement. Atom model of the final substrate coordinates is shown with all bond lengths (Å), including esd's in parentheses. Values were determined by least-squares refinement without use of any geometric restraints. (**C**) Schiff base intermediate. Same view as above for the DERA K201L mutant. In this complex, the Schiff base formation is observed as indicated by the shorter Lys^{167}-Nζ to C1 bond length and loss of the hydroxyl group. Wat^{29} in the carbinolamine complex (B) is equivalent to Wat^{21} in the Schiff base complex (C) (*24*). Below, refined parameters for the Schiff base complex from unrestrained refinement, as above in (B).

panaldehyde and (*S*)-2-deuteropropanaldehyde (*39*) in D_2O, the pro*S* proton is exchanged in both cases (Fig. 4A). Hence, the DERA-catalyzed aldol reaction between propanal and D-3-azido-2-propanal proceeds with retention of configuration at C2, so that the exchanging proton and the aldehyde approach the same face of the enzyme-bound enamine (Fig. 4C) (*40*).

In the crystal structures of either the wild-type carbinolamine complex (Figs. 2B and 3A) or of the K201L mutant of DERA in a Schiff base complex with DRP (Figs. 2C and 3B), no protein side chain is close enough to C2 to suggest direct participation in the reaction mechanism. The closest residues, other than Lys^{167}, are Lys^{201}, Asp^{102}, and Cys^{47} (Fig. 3), for which their respective side-chain heteroatoms are 5.3, 5.3, and 5.5 Å, respectively, from the C2 of DRP in the carbinolamine complex. Therefore, barring an unobserved and unexpected (from modeling studies) conformational change, none of these residues are good general base candidates. The closest heteroatom to C2 of DRP, which is observed in all the DERA structures to date, is an extensively hydrogen-bonded water molecule (Wat^{29}, Fig. 3A) (*24*) which is 3.95 Å from DRP C2 [see Web table 2B (*22*)], about 0.7 Å too far away to be unambiguously assigned to the role of general base from the structural data. Consequently, we turned to molecular mechanics analysis to investigate flexibility in the active site. Minimization of the wild-type carbinolamine structure produced little change, validating the results of the minimization method with the observed structural data (*37*). For Asp^{102}, Lys^{201}, Cys^{47}, or Wat^{29}, the distances between the side-chain heteroatom and C2 were altered by less than 0.1 Å. However, when the DERA-acetaldehyde enamine intermediate was minimized, the oxygen atom of Wat^{29} moved to within 3.26 Å from C2, whereas Asp^{102}, Lys^{201}, and Cys^{47} remained at least 5 Å away from C2 [see Web table 2B (*22*)].

Thus, we propose that this water molecule participates in a proton relay (Fig. 4B) by which C2 is stereoselectively deprotonated. The effective tautomerization of the enzyme acetaldehyde imine to its enamine, as shown in step 3 of Fig. 4B, is catalyzed via this proton relay system that involves Asp^{102} and Lys^{201}. The fact that the K201L, K201R, $Asp^{102} \rightarrow Leu^{102}$ (D102L), and $Asp^{102} \rightarrow Asn^{102}$ mutants all exhibit 10^3 times less activity than the wild type corroborates this hypothesis. Furthermore, the $Asp^{102} \rightarrow Glu^{102}$ mutant, which retains a carboxyl side chain, can still catalyze the retroaldol reaction, albeit at a 45-fold reduced rate. This mutant also retains the ability to catalyze the C2 exchange, as shown by ^1H NMR (Table 2), because it can still participate in proton shuffling.

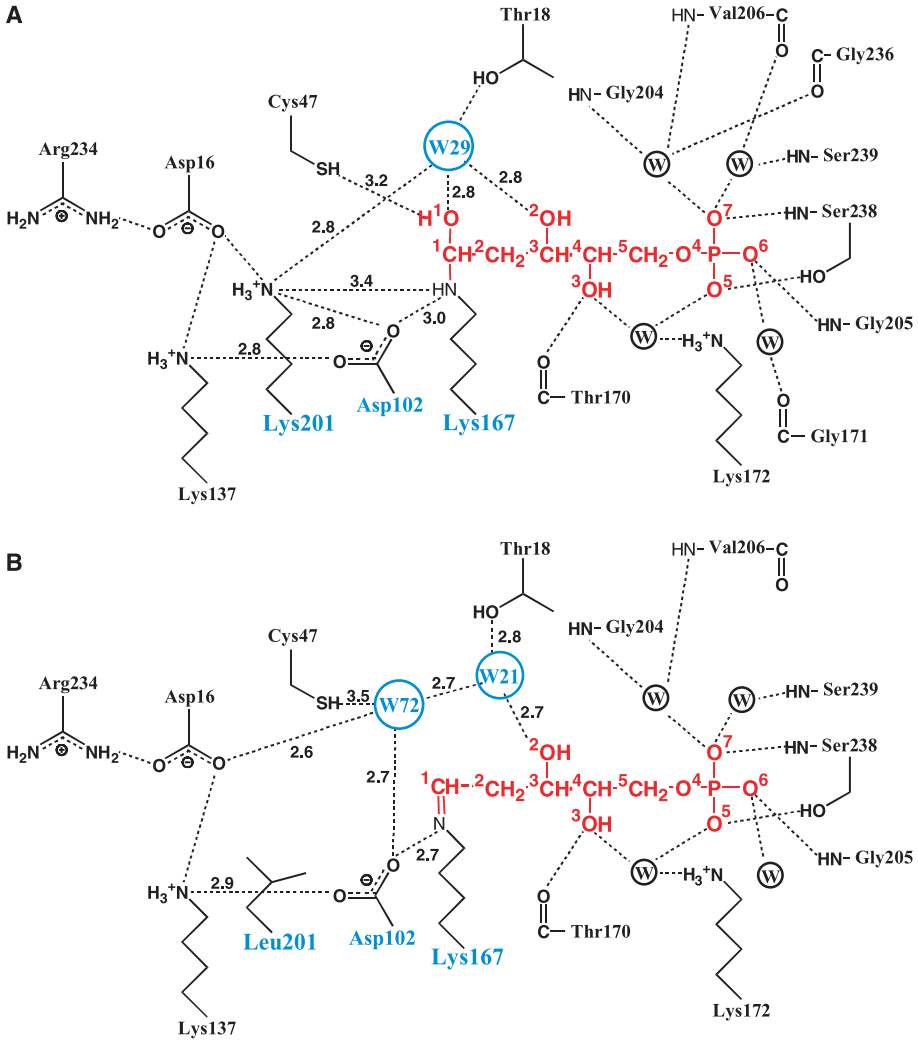

Fig. 3. DERA enzyme-substrate interactions. The wild-type enzyme carbinolamine complex (**A**) and the Schiff base K201L mutant complex (**B**) structures are shown. Residues and water molecules implicated in catalysis are colored in blue. The different covalent intermediates observed in each structure are colored in red. Hydrogen bonds are indicated by dotted black lines and lengths are given in angstroms. Carbon and oxygen atoms are numbered in DRP, as in Fig. 2, B and C.

Identification of the general base responsible for C2 proton abstraction may have remained elusive in type I aldolases because it functions via an extensive proton relay in a fashion analogous to that proposed for pyruvate kinase (*41*). The detailed catalytic mechanism as outlined in Fig. 4B is for the DERA enzyme. However, other class I aldolase enzymes contain similar constellations of residues that could function in proton relay systems analogous to DERA. Although Asp^{33} and Glu^{45} have been proposed to function as the general base in FBP and KDPG aldolases, the available substrate complex structures are not consistent with this postulate (*7*, *15*-*19*).

Thus, we can now put forward a complete mechanism for a type I aldolase, which delineates all of the essential catalytic residues (Fig. 4B) and is consistent with all of our ultra–high resolution structural, site-directed mutagenesis and ^1H NMR data. Lys^{167} is identified as the Schiff base–forming residue. After the enamine is formed, the system is poised for nucleophilic attack onto the acceptor aldehyde D-glyceraldehyde-3-phosphate, requiring protonation of its carbonyl group. From the ultra–high resolution structures (Fig. 2, B and C) and modeling, it appears that this proton is provided via Wat^{29} [Web table 2B (*22*)] through a proton relay that is composed of Asp^{102}, Lys^{201}, and the active-site water molecule, and is responsible for shuffling a proton between C2 of the acetaldehyde imine and enamine and subsequent C3 hydroxyl protonation (Fig. 4B). In addition to the relevance for class I aldolase mechanisms, these results may have implications

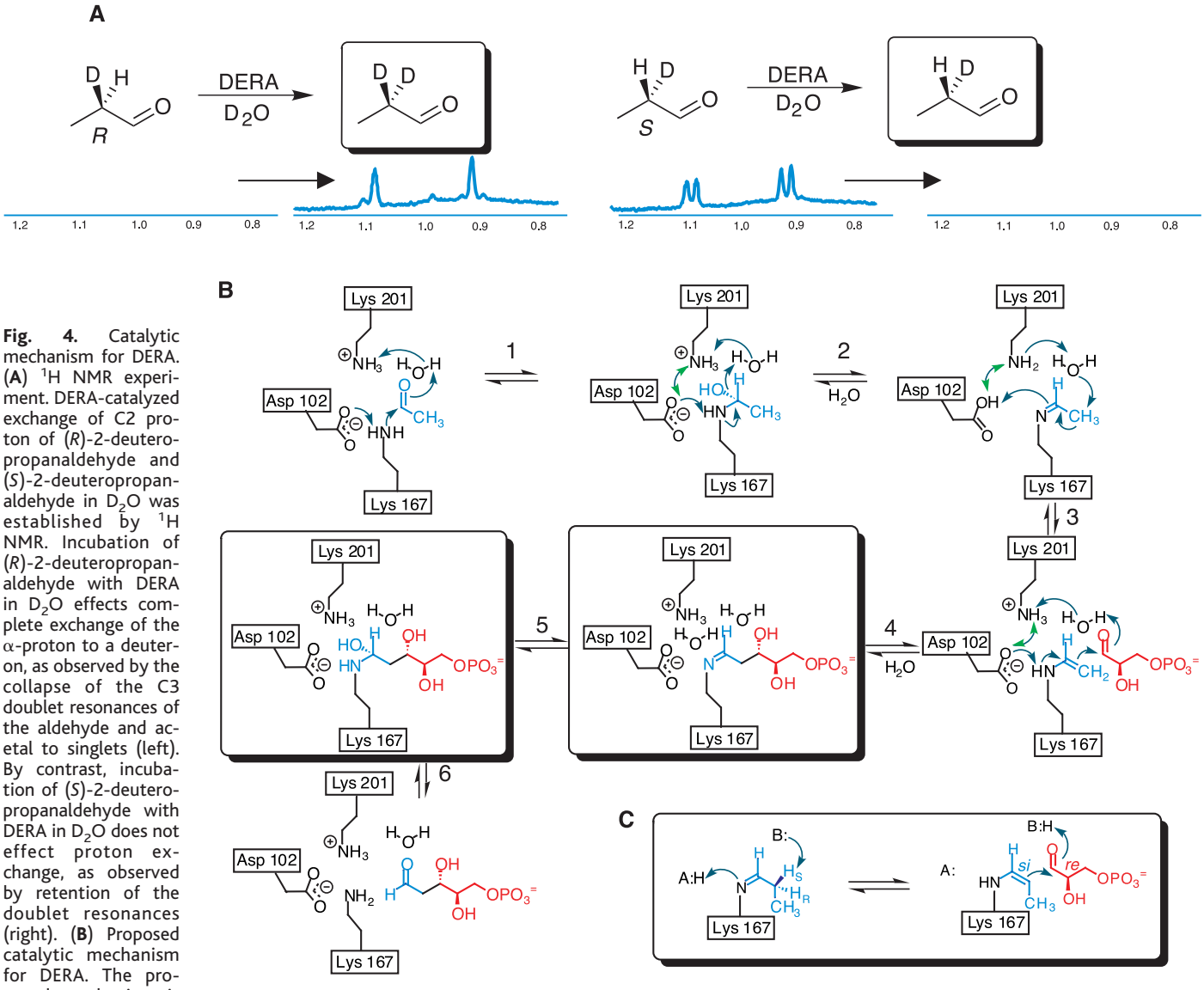

Fig. 4. Catalytic mechanism for DERA. (**A**) ^{1}H NMR experiment. DERA-catalyzed exchange of C2 proton of (*R*)-2-deuteropropanaldehyde and (*S*)-2-deuteropropanaldehyde in D_2O was established by ^{1}H NMR. Incubation of (*R*)-2-deuteropropanaldehyde with DERA in D_2O effects complete exchange of the α-proton to a deuteron, as observed by the collapse of the C3 doublet resonances of the aldehyde and acetal to singlets (left). By contrast, incubation of (*S*)-2-deuteropropanaldehyde with DERA in D_2O does not effect proton exchange, as observed by retention of the doublet resonances (right). (**B**) Proposed catalytic mechanism for DERA. The proposed mechanism is consistent with all of our ultra–high resolution structural, modeling, site-directed mutagenesis, and ^{1}H NMR data. Lys^{167} is identified as the Schiff base–forming residue. After the enamine is formed, the system is poised for nucleophilic attack onto the carbonyl-carbon of the acceptor aldehyde D-glyceraldehyde-3-phosphate. A proton relay system between Asp^{102}, Lys^{201}, and an active site water molecule is responsible for shuffling a proton between C2 of the acetaldehyde imine and enamine and subsequent C3 hydroxyl protonation. The double arrows in green indicate rapid proton shuffling between Lys^{201} and Asp^{102}. Crystallographically observed reaction intermediates are boxed (left, carbinolamine; right, Schiff base). (**C**) Stereochemical course of aldol reaction. When propanal is substituted for acetaldehyde as the donor, the *pro-S* α proton is removed, and thus the aldol reaction proceeds with retention of configuration at C2, with the *Si* face of the resulting enamine approaching the *Re* face of the acceptor carbonyl. A:H, general acid; B, general base.

regarding the prevailing mechanistic views of other Schiff base–forming enzymes, such as carboxylases and transaminases.

References and Notes

1. P. Valentin-Hansen, F. Boetius, K. Hammer-Jespersen, I. Svendsen, *J. Biochem.* **125**, 561 (1982).
2. I. A. Rose, E. L. O'Connell, *Arch. Biochem. Biophys.* **118**, 758 (1967).
3. W. E. Pricer Jr., B. L. Horecker, *J. Biol. Chem* **5**, 1292 (1960).
4. P. Hoffee, P. Snyder, C. Sushak, P. Jargiello, *Arch. Biochem. Biophys.* **164**, 736 (1974).
5. C. F. Barbas III, Y.-F. Wang, C.-H. Wong, *J. Am. Chem. Soc.* **112**, 2013 (1990).
6. S. Fong, T. D. Machajewski, C. C. Mak, C.-H. Wong, *Chem. Biol.* **7**, 873 (2000).
7. K. H. Choi *et al.*, *Biochemistry* **38**, 12655 (1999).
8. T. D. Machajewski, C.-H. Wong, *Angew. Chem. Int. Ed.* **39**, 1352 (2000).
9. M. Silvestri, G. DeSantis, C.-H. Wong, *Topics Stereochem.*, in press.
10. J. Wagner, R. A. Lerner, C. F. Barbas III, *Science* **270**, 1797 (1995).
11. C. F. Barbas III *et al.*, *Science* **278**, 2085 (1997).
12. G. Zhong *et al.*, *Angew. Chem. Int. Ed.* **37**, 2481 (1998).
13. G. Zhong, R. A. Lerner, C. F. Barbas III, *Angew. Chem. Int. Ed. Engl.* **38**, 3738 (1999).
14. A. Karlstrom *et al.*, *Proc. Natl. Acad. Sci. U.S.A.* **97**, 3878 (2000).
15. N. Wymer *et al.*, *Structure* **9**, 1 (2001).
16. H. P. Meloche, J. P. Glusker, *Science* **181**, 350 (1973).
17. J. Allard, P. Grochulski, J. Sygusch, *Proc. Natl. Acad. Sci. U.S.A.* **98**, 3679 (2001).
18. C. L. Verlinde, P. M. Quigley, *J. Mol. Model* **5**, 37 (1999).
19. A. Dalby, Z. Dauter, J. A. Littlechild, *Protein Sci.* **8**, 291 (1999).
20. N. Blom, J. Sygusch, *Nature Struct. Biol.* **4**, 36 (1997).
21. J. Jia, U. Schoerken, Y. Lindqvist, G. A. Sprenger, G. Schneider, *Protein Sci.* **6**, 119 (1997).
22. Supplementary Web material is available on *Science* Online at www.sciencemag.org/cgi/content/full/294/5541/369/DC1.
23. The phosphate group is located near the NH_2-terminus of the last helix of the molecule and is in main-chain contact with N-Ser^{238} and Gly^{205} and via a water molecule with Gly^{204}, Val^{206}, Ser^{239}, and Gly^{171}. Lys^{172} presumably provides a countercharge for the phosphate group in addition to the dipole moment of the α helix (*42*).
24. This water, Wat^{29}, is structurally conserved in all DERA structures and has a very low B value of 11.4 Å^2 for molecule 1 and 12.6 Å^2 for molecule 2, respectively. Superposition of the carbinolamine with the

Schiff base complex shows that Wat[21] is equivalent to Wat[29]. Also in the native structure, a water molecule is found in the identical position (within 0.5 Å of Wat[29] of the carbinolamine). Wat[72] in the Schiff base complex could correspond to the water molecule derived from protonation of the hydroxyl group of the carbinolamine.

25. Known class I structures used for comparison were KDPG aldolase in complex with pyruvate [Protein Data Bank (PDB) code 1EUA] (*17*), human muscle fructose 1,6-bisphosphate aldolase (PDB code 4ALD) (*19*), rabbit muscle 1,6-bisphosphate fructose aldolase (PDB code 1ADO) (*20*), and transaldolase B (PDB code 1UCW) (*21*).
26. This mutant crystallized under the same conditions as the wild type, and the substrate soak was repeated as reported in Table 1.
27. This observation was also made for the rabbit aldolase A, where the Lys[146] → Arg[146] mutant retained the ability to form the Schiff base intermediate (*43*).
28. F. H. Westheimer, D. E. Schmidt Jr., *Biochemistry* **10**, 1249 (1971).
29. F. H. Westheimer, *Tetrahedron* **51**, 3 (1995).
30. Experimental conditions for the pH activity profile were as follows: 25 mM buffer solutions of sodium formate (pH 3.5, 3.0, and 4.0); sodium acetate (pH 4.5, 5.0, and 5.5); MES (pH 5.5, 6.0, and 6.5); MOPS (pH 6.5, 7.0, and 7.5); tetraethylammonium-chloride (TEA-HCl) (pH 7.5, 8.0, and 8.5); CAPSO (pH 8.5, 9.0, and 9.5), and CAPS (pH 10, 10.5, and 11.0). V_{max} was measured from pH 4 to 10 in the retroaldol direction with 3 mM DRP in 50 mM (pH 7.5) TEA-HCl buffer in the presence of 0.3 mM reduced nicotinamide adenine dinucleotide (NADH) using a glyceraldehyde 3-phosphate dehydrogenase/triosephosphate isomerase (GPD/TPI)–coupled (5.3 U/ml, Sigma G-1881) enzyme system at 25°C by observing the rate of decrease of NADH concentration as monitored at 340 nm (*44*).
31. In rabbit aldolase A, the equivalent Lys[146] residue has been implicated as being involved in cleavage and condensation of the C3–C4 bond of fructose 1,6-bisphosphate (*45*), in addition to lowering the pK_a of Lys[229].
32. All solvent-accessible surface areas were calculated with the program MS (*46*) with a 1.4 Å probe sphere and standard atomic radii (*47*).
33. Experimental conditions for the Schiff base trapping experiment were as follows: DERA (1 mg/ml) was incubated with 5 mM acetaldehyde in 20 mM TEA-HCl, 50 mM NaCl, and 2 mM $CaCl_2$ (pH 7.4) at 22°C for 10 min. Fifty mM $NaBH_4$ was added, and incubation continued for 12 hours. Samples were dialyzed against dH_2O and then purified by high-performance liquid chromatography on a C18 column before analysis by electrospray ionization mass spectrometry (with a Perkin Elmer API III Sciex triple quadrupole). Observed masses agreed within ±4 daltons to theoretical values.
34. A. Heine, J. G. Luz, C.-H. Wong, I. A. Wilson, in preparation.
35. J. A. Littlechild, H. C. Watson, *Trends Biochem. Sci.* **18**, 36 (1993).
36. The activity of the class I aldolase from halophilic archaebacterium *Haloarcula vallismortis* was not affected by carboxypeptidase digestion (*48*).
37. The model was constructed with Molecular Simulations Insight 2000. Setup was as described (*49*). The CVFF force field provided in the Discover module of InsightII was used.
38. C. F. Barbas III, thesis, Texas A&M University, College Station, TX (1989).
39. Experimental conditions for deuteropropanal synthesis and the DERA exchange experiment were as follows: (*R*)-2-deuteropropanol was synthesized from (*S*)-(+)-1,2-propanediol as described in (*50*) with minor modification. ^{1}H NMR ($CDCl_3$, 500 MHz): 3.62 (d, J = 6.97 Hz, 2H), 1.60 to 1.55 (m, 1H), 0.91 (d, J = 7.34 Hz, 3H). ^{13}C NMR ($CDCl_3$, 125 MHz): 64.58, 24.79 (t, J = 20 Hz), 9.91. (*R*)-2-deuteropropanol: $[\alpha]_D$ = +1.11°, ($CDCl_3$, c = 0.18); lit. +0.06°, (neat). (*S*)-2-deuteropropanol was prepared analogously: $[\alpha]_D$ = −0.05° ($CDCl_3$, c = 1.8); lit. −0.06° (neat). In an NMR tube, (*R*)- or (*S*)-2-deuteropropanol was incubated at 0.4 mM in 100 mM TEA-HCl buffer made up with D_2O together with 8 mM pyruvic acid, 1 mM NAD^+, yeast alcohol dehydrogenase (0.25 mg/ml) (82.5 U), and L-lactic dehydrogenase (0.25 mg/ml) (214.5 U), pH in D_2O (pD) = 7.1. After the oxidation of deuteropropanol to deuteropropanal was deemed substantially complete by the appearance of the aldehyde C3 resonance by ^{1}H NMR (D_2O, 500 MHz): 1.08 (d, J = 7.34 Hz, 3H), then 0.5 mg/ml (50 U) wild-type DERA was added. For (*R*)-2-deuteropropanal, this resonance collapses to a singlet 1.04 (s, 3H) after 3 hours, whereas for (*S*)-2-deuteropropanal it remains unchanged.
40. L. Chen, D. P. Dumas, C.-H. Wong, *J. Am. Chem. Soc.* **114**, 741 (1992).
41. T. M. Larsen, M. M. Benning, I. Rayment, G. H. Reed, *Biochemistry* **37**, 6247 (1998).
42. R. R. Copley, G. J. Barton, *J. Mol. Biol.* **242**, 321 (1994).
43. A. J. Morris, R. C. Davenport, D. R. Tolan, *Prot. Eng.* **9**, 61 (1996).
44. P. C. Nicholas, *Biochem. Soc. Trans.* **16**, 752 (1988).
45. A. J. Morris, D. R. Tolan, *Biochemistry* **33**, 12291 (1994).
46. M. L. Connolly, *J. Appl. Crystallogr.* **16**, 439 (1983).
47. S. Sheriff, *Immunomethods* **3**, 191 (1993).
48. G. Krishnan, W. Altekar, *Eur. J. Biochem.* **195**, 343 (1991).
49. G. DeSantis, J. B. Jones, *J. Am. Chem. Soc.* **120**, 8582 (1998).
50. M. M. Green, J. M. Moldowan, J. G. McGrew II, *J. Org. Chem.* **39**, 2166 (1974).
51. Z. Otwinowski, W. Minor, *Methods Enzymol.* **276A**, 307 (1997).
52. A. T. Brünger *et al.*, *Acta Crystallogr. D* **54**, 905 (1998).
53. G. M. Sheldrick, T. R. Schneider, *Methods Enzymol.* **277B**, 319 (1997).
54. T. A. Jones, J. Y. Zou, S. W. Cowan, M. Kjeldgaard, *Acta Crystallogr. A* **47**, 110 (1991).
55. H. Kim, U. Certa, H. Dobeli, P. Jakob, W. G. Hol, *Biochemistry* **37**, 4388 (1998).
56. J. Sygusch, D. Beaudry, M. Allaire, *Proc. Natl. Acad. Sci. U.S.A.* **84**, 7846 (1987).
57. R. A. Laskowski, M. W. MacArthur, D. S. Moss, J. M. Thornton, *J. Appl. Crystallogr.* **26**, 283 (1993).
58. P. C. Nicholas, *Biochem. Soc. Trans.* **16**, 752 (1988).
59. Experimental conditions for propanal exchange with DERA mutants were as follows: In an NMR tube, propropanal was incubated at 200 mM in 100 mM TEA-HCl buffer made up with D_2O (pD = 7.1) and DERA (2 mg/ml) was added (50 U for wild-type DERA). Samples were analyzed by ^{1}H NMR (D_2O, 250 MHz). For wild-type DERA, the C3-aldehyde triplet resonance 1.03 (t, J = 7.01 Hz, 3H) collapses to a doublet 1.02 (d, J = 7.3 Hz, 3H).
60. P. J. Kraulis, *J. Appl. Crystallogr.* **24**, 946 (1991).
61. E. A. Merritt, D. J. Bacon, *Methods Enzymol.* **277**, 505 (1997).
62. We gratefully acknowledge helpful discussions with F. Huang, S. Fong, L. Lee, T. Tolbert, P. Sears, W. W. Cleland, G. M. Sheldrick, J. H. Naismith, and R. A. Lerner. Supported by NIH grants GM44154 (C.H.W.) and CA27489 (I.A.W.), a Natural Science and Engineering Research Council of Canada postdoctoral fellowship (G.D.), and a UNCF-Merck Science Initiative fellowship (M.M.). We thank the Stanford Synchrotron Radiation Laboratory staff of beamline 9-2, X. Dai, and S. E. Greasley for help with data collection and processing, and M. Elsliger for computational assistance. This is publication 14200-MB from the Scripps Research Institute. The coordinates have been deposited in the PDB with access codes 1JCL (wild-type DERA) and 1JCJ (K201L mutant of DERA) and are available immediately from aheine@scripps.edu.

19 June 2001; accepted 2 August 2001

Carboxyl-Terminal Modulator Protein (CTMP), a Negative Regulator of PKB/Akt and v-Akt at the Plasma Membrane

Sauveur-Michel Maira,[1] Ivana Galetic,[1] Derek P. Brazil,[1] Stefanie Kaech,[1]* Evan Ingley,[1]† Marcus Thelen,[2] Brian A. Hemmings[1]‡

The PKB (protein kinase B, also called Akt) family of protein kinases plays a key role in insulin signaling, cellular survival, and transformation. PKB is activated by phosphorylation on residues threonine 308, by the protein kinase PDK1, and Serine 473, by a putative serine 473 kinase. Several protein binding partners for PKB have been identified. Here, we describe a protein partner for PKBα termed CTMP, or carboxyl-terminal modulator protein, that binds specifically to the carboxyl-terminal regulatory domain of PKBα at the plasma membrane. Binding of CTMP reduces the activity of PKBα by inhibiting phosphorylation on serine 473 and threonine 308. Moreover, CTMP expression reverts the phenotype of v-*Akt*–transformed cells examined under a number of criteria including cell morphology, growth rate, and in vivo tumorigenesis. These findings identify CTMP as a negative regulatory component of the pathway controlling PKB activity.

PKB is a major downstream target of receptor tyrosine kinases that signal via the phosphatidylinositol 3-kinase (PI 3-kinase). PKB mediates a wide variety of biological responses to insulin and insulin-like growth factor 1 (IGF-1) and other growth factors (*1*–*2*). Upon cell stimulation, the kinase is translocated to the plasma membrane, where it is phosphorylated on two amino acids, Thr[308] in the catalytic domain and Ser[473] in the COOH-

ERRATUM

post date 7 December 2001

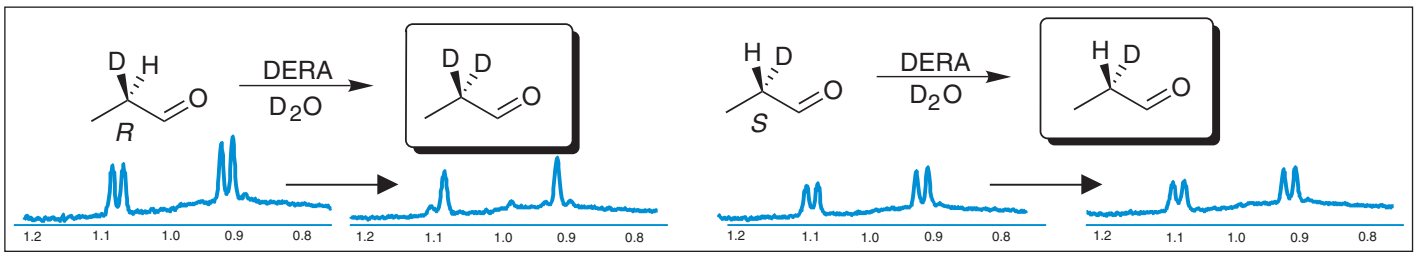

REPORTS: "Observation of covalent intermediates in an enzyme mechanism at atomic resolution" by A. Heine *et al.* (12 Oct. 2001, p. 369). In Fig. 4A, two of the four ^{1}H nuclear magnetic resonance spectra did not print. The correct figure panel appears here.